NRC Research Press

ARTICLE

Sands subjected to repetitive vertical loading under zero lateral strain: accumulation models, terminal densities, and settlement

Song-Hun Chong and J. Carlos Santamarina

Abstract: Geosystems often experience numerous loading cycles. Plastic strain accumulation during repetitive mechanical loads can lead to shear shakedown or continued shear ratcheting; in all cases, volumetric strains diminish as the specimen evolves towards terminal density. Previously suggested models and new functions are identified to fit plastic strain accumulation data. All accumulation models are formulated to capture terminal density (volumetric strain) and either shakedown or ratcheting (shear strain). Repetitive vertical loading tests under zero lateral strain conditions are conducted using three different sands packed at initially low and high densities. Test results show that plastic strain accumulation for all sands and density conditions can be captured in the same dimensionless plot defined in terms of the initial relative density, terminal density, and ratio between the amplitude of the repetitive load and the initial static load. This observation allows us to advance a simple but robust procedure to estimate the maximum one-dimensional settlement that a foundation could experience if subjected to repetitive loads.

Key words: long-term soil response, drained repetitive loads under zero lateral strain, plastic strain accumulation models, one-dimensional settlement.

Résumé : Les géosystèmes subissent souvent de nombreux cycles de chargement. Une accumulation de déformation plastique lors de sollicitations mécaniques répétitives peut conduire à un cisaillement par secouage ou un cisaillement continue par cliquet; dans tous les cas, les déformations volumétriques diminuent à mesure que l'échantillon évolue vers la densité terminale. Les modèles auparavant suggérés et les nouvelles fonctions sont identifiés en fonction des données d'accumulation de déformation plastique. Tous les modèles d'accumulation sont formulés pour capturer la densité terminale (déformation volumique) et soit un secouage ou un cliquet (déformation par cisaillement). Des essais de chargement vertical répétitif sous zéro condition de déformation latérale sont effectués en utilisant trois différents sables emballés à des densités initialement basses et hautes. Les résultats d'essais montrent que l'accumulation de déformation plastique pour tous les sables et les conditions de densité peut être capturée dans la même parcelle non dimensionnée définie en termes de la densité relative initiale, la densité terminale, et le rapport entre l'amplitude de la charge répétitive et la charge statique initiale. Cette observation nous permet d'avancer une procédure simple, mais robuste pour estimer le tassement unidimensionel maximal qu'une fondation pourrait subir si elle est soumise à des charges répétitives. [Traduit par la Rédaction]

Mots-clés : réponse du sol à long terme, charges répétitives drainées sous zéro déformation latérale, modèles d'accumulation de déformation plastique, tassement unidimensionel.

Introduction

The study of repetitive loads has been advanced in the context of pavements, railroads, runways, earthquakes, and machine foundations (early studies by D'Appolonia et al. 1969; Silver and Seed 1971; Barksdale 1972; Youd, 1972; Brown 1974, 1996; Monismith et al. 1975; Lentz and Baladi 1980; Lentz and Baladi 1981; Diyaljee and Raymond 1982; and more recently Li and Selig 1996; Chai and Miura 2002; Abdelkrim et al. 2003; Suiker and de Borst 2003; Ishikawa et al. 2011). Renewed attention is driven by the long-term response of energy-related geostructures, such as the foundations of wind turbines, compressed air energy storage, and energy piles (Yeo et al. 1994; Niemunis et al. 2005; Laloui et al. 2006; Morgan and Ntambakwa 2008; Achmus et al. 2009; Pasten and Santamarina 2011; Pasten et al. 2014; Sánchez et al. 2014). Indeed, published data show that geomaterials may experience significant strains as they undergo "mechanical cycles" (Luong 1980; Sawicki, 1994; Sawicki and Swidzinski 1995; Wichtmann et al. 2005, 2010*b*), "thermal cycles" (Viklander 1998; Chen et al. 2006), and either "suction or chemical cycles" (Osipov et al. 1987; Pejon and Zuquette 2002; Tripathy and Subba Rao 2009).

The main purposes of this study are to (*i*) summarize salient features of soil behavior when subjected to repetitive mechanical loads, (*ii*) identify plastic strain accumulation functions that can be expressed in terms of a small number of physically meaningful parameters, (*iii*) investigate the evolution of volumetric strain induced by repetitive vertical loading under zero lateral strain, and (*iv*) suggest a methodology to estimate the maximum settlement based on terminal density.

Previous studies — salient observations

Plastic strain accumulation in soils subjected to repetitive loads depends on the soil type and density, initial effective stress, cyclic

Received 20 January 2016. Accepted 9 August 2016.

S.-H. Chong. Civil and Environmental Engineering, KAIST, Deajeon 305-701, South Korea.
J.C. Santamarina. Earth Science and Engineering, KAUST, Thuwal 23955-6900, Saudi Arabia.
Corresponding author: Song-Hun Chong (email: songhun.chong@gmail.com).

Table 1. Generalized plastic strain accumulation functions for volumetric and deviatoric strains.

Type	Strain accumulation function	Plastic strain accumulation rate in the *i*th cycle	Asymptotic conditions for $i \to \infty$: For volumetric strain	Asymptotic conditions for $i \to \infty$: For shear strain	Related references
Exponential function	$\varepsilon_i^{acc} = \varepsilon_1 + b\{1 - \exp[-c(i-1)]\} + d(i-1)$	$\frac{d\varepsilon_i^{acc}}{di} = bc\exp[-c(i-1)] + d$	$b = \varepsilon_\infty - \varepsilon_1$ and $d = 0$ (terminal density)	Shakedown $d = 0$ ratcheting $d > 0$	Wolff and Visser (1994); Knight et al. (1995); Rosato and Yacoub (2000); Chen et al. (2006); Narsilio and Santamarina (2008)
Hyperbolic function	$\varepsilon_i^{acc} = \varepsilon_1 + b\frac{i^c - 1}{i^c + b} + d(i-1)$	$\frac{d\varepsilon_i^{acc}}{di} = \frac{bci^c(b+1)}{i(b+i^c)^2} + d$	$b = \varepsilon_\infty - \varepsilon_1$ and $d = 0$ (terminal density)	Shakedown $d = 0$ ratcheting $d > 0$	Inspired by Kondner (1963); Duncan and Chang (1970)
Polynomial function	$\varepsilon_i^{acc} = \varepsilon_1 + b(1 - i^c) + d(i-1)$	$\frac{d\varepsilon_i^{acc}}{di} = bci^{-(1+c)} + d$	$b = \varepsilon_\infty - \varepsilon_1$ and $d = 0$ (terminal density)	Shakedown $d = 0$ ratcheting $d > 0$	Paute et al. (1996); see Lekarp et al. (1996)
Power function	$\varepsilon_i^{acc} = \varepsilon_1 + b(i^c - 1) + d(i-1)$	$\frac{d\varepsilon_i^{acc}}{di} = bci^{c-1} + d$	Requires shutoff	Shakedown requires shutoff ratcheting $d > 0$	Monismith et al. (1975); Diyaljee and Raymond (1982); Monismith et al. (1994); Brown (1996); Lekarp et al. (1996); Li and Selig (1996); Dennis et al. (1999); Chai and Miura (2002)
Log-linear function	$\varepsilon_i^{acc} = \varepsilon_1 + b\log(i) + d(i-1)$	$\frac{d\varepsilon_i^{acc}}{di} = \frac{b}{\ln(10)}(i)^{-1} + d$	Requires shutoff	Shakedown requires shutoff ratcheting $d > 0$	Lentz and Baladi (1980); Stewart (1986); Sawicki and Swidzinski (1995); Brown (1996); Niemunis et al. (2005); François et al. (2010); Karg et al. (2010); Pasten et al. (2014)

Note: All equations apply for $i \geq 1$. As presented, ε_1 and fitting parameters b, c, and d are greater than or equal to zero. The last term in all equations is added to capture shear ratcheting: the d factor is the rate of ratcheting for $i \gg 1$. In terms of void ratio, the accumulated volumetric strain after the ith cycle is $\varepsilon_i^{acc} = \frac{e_{i=o} - e_i}{1 + e_{i=o}}$.

Table 2. Materials used in this study.

Sand	Gs	Particle shape: R	Particle shape: S	Extreme void ratios: e_{max}	Extreme void ratios: e_{min}
Blasting	2.65	0.50	0.50	1.03	0.70
Ottawa F110	2.65	0.70	0.70	0.95	0.56
Ottawa 50–70	2.65	0.90	0.70	0.86	0.55

Note: Gs, specific gravity; R, roundness; S, sphericity (refer to Cho et al. 2006). Maximum and minimum void ratios are measured according to ASTM (2014) D4253 (e_{min}) and ASTM (2014) D4254 (e_{max}).

stress amplitude and obliquity, and number of cycles (Barksdale 1972; Brown 1974; Diyaljee and Raymond 1982; Stewart 1986; Chang and Whitman 1988; Kaggwa et al. 1991; Wichtmann et al. 2007, 2010*a*; Karg et al. 2010).

Particle-scale simulations show rapid fabric rearrangement during early cycles and contact sliding as the main mechanisms for irreversible deformation (Alonso-Marroquin and Herrmann 2004; García-Rojo and Herrmann, 2005). Strain accumulation evolves towards asymptotic conditions as the number of cycles increases, $i \gg 1$. Asymptotic trends for volumetric and shear strains are described next.

Volumetric strain: terminal void ratio

A soil will reach a terminal void ratio and characteristic fabric for any sustained process it is subjected to, including repetitive loading (Narsilio and Santamarina 2008; see early reference to the term in D'Appolonia and D'appolonia 1967). At terminal void ratio, the net volume change per cycle is zero and the soil ceases to accumulate volumetric deformation. While volumetric contraction is most common in soils subjected to repetitive loading, dilative soils strained significantly beyond their contraction–dilation transition point — or "characteristic state" — will experience disruption of interlocking and will dilate as they evolve towards terminal density (Monismith et al. 1975; Luong 1980; Wichtmann et al. 2005). Evolution towards terminal density is accompanied by changes in horizontal stress when soils experience cyclic vertical loads under zero lateral strain boundary conditions (D'Appolonia et al. 1969; Finn and Vaid 1977; Finn 1981; Bouckovalas et al. 1984; Sawicki 1994; Sawicki and Swidzinski 1995; Wichtmann et al. 2010*a*).

Shear strain: shakedown and ratcheting

Shear strain accumulation exhibits a wider range of asymptotic conditions. Based on previous studies on repetitive loads, analysis of soil fabric, and measurements of energy losses, the following stages are identified (Koiter 1960; Barksdale 1972; Brown 1974; Sawczuk 1974; Monismith et al. 1975; Sharp and Booker 1984; Alonso-Marroquin and Herrmann 2004; García-Rojo and Herrmann 2005):

- *Viscoelastic shakedown* — In this regime, shear strains stop accumulating, there is no creation or loss of interparticle contacts, and there is no contact slippage; yet, energy is dissipated in every cycle (e.g., fluid-skeleton viscous losses in wet sands, and thermoelastic losses in dry sands; Wang and Santamarina 2007).
- *Plastic shakedown* — The strain level in each cycle exceeds the elastic threshold strain, there is contact slippage and particle rearrangement in every cycle, and energy dissipation involves frictional loss; yet, there is no accumulation of residual shear strain at the end of the cycle.
- *Ratcheting* — Plastic shear strains continue accumulating in every cycle. While interparticle contacts change in every cycle, statistical fabric descriptors such as polar plots of contacts and contact forces evaluated at the end of every cycle converge towards constant asymptotic conditions after a large number of cycles.

Fig. 1. Void ratio evolution during "monotonic–repetitive–monotonic" loading under zero lateral strain boundary conditions for (*a*) blasting sand, (*b*) Ottawa F110 sand, and (*c*) Ottawa 50–70 sand. Data are presented for three soils packed at two different relative densities, and subjected to two different levels of initial stress (total of 12 tests). The amplitude of the applied repetitive load is 100 kPa in all cases. Data extracted around the repetitive load stage are shown for each test; thus, each plot shows four different tests. Complementary monotonic test results overlap on these trends (not shown for clarity). [Color online.]

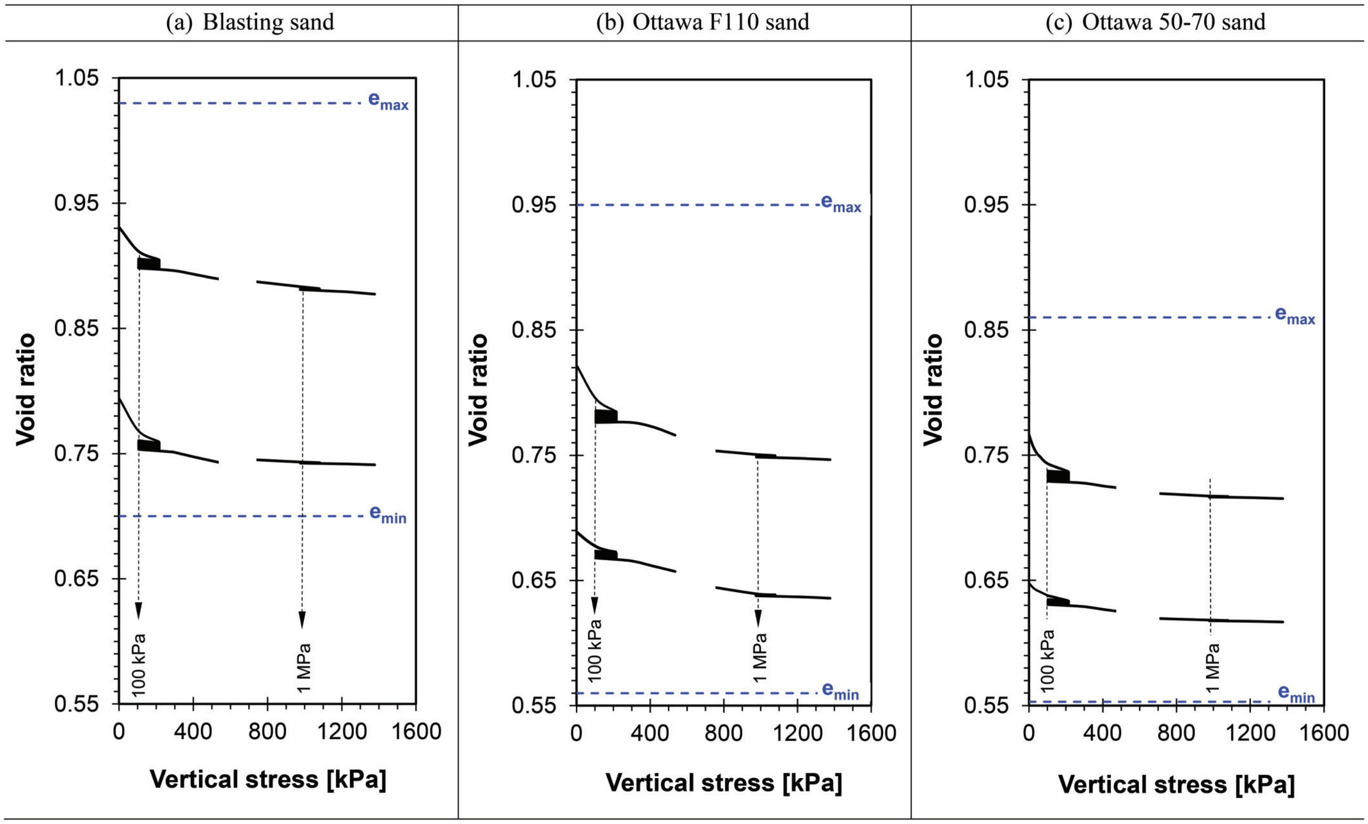

Other observations: varying load sequences

Cumulative damage models have been proposed to estimate the long-term material response under varying load cycles. (Note: see Fatemi and Yang 1998 for a review of damage models in cohesive media.) Experimental results obtained with freshly remolded sands in drained triaxial tests show that the linear model known as Miner's rule adequately accumulates plastic strains caused by repetitive loads of varying amplitudes (Kaggwa et al. 1991; Wichtmann et al. 2010*a*).

Plastic strain accumulation models

Strain accumulation functions are used to model the evolution of permanent deformations that soils experience under repetitive loading. Previously suggested and new plastic strain accumulation functions are compiled in Table 1. The functions are generalized to model either volumetric or shear strains, and to capture their asymptotic conditions, such as terminal density, shakedown, and ratcheting (i.e., linear accumulation at a large number of cycles). In all cases, functions are written in terms of the plastic strain at the end of the first cycle, $\varepsilon_{i=1}$.

Exponential function

The salient property of the exponential function is that the instantaneous rate of change is defined by the current state. This four-parameter model can be matched to volumetric strain data or to shear strain data where shakedown response implies fitting parameter $d = 0$ and ratcheting $d > 0$.

Hyperbolic model

Hyperbolic-type models are defined by an initial tangent and an ultimate asymptote. The generalized four-parameter hyperbolic model presented in Table 1 can capture the volumetric and shear plastic strain accumulation; in particular, the rate of densification can be adjusted with the c exponent.

Polynomial function and power model

For clarity, two separate expressions are included in Table 1 where model parameters are assumed to be positive numbers (Note: the polynomial function is mathematically equivalent to the power model when negative b and c values are used.) When positive-valued parameters are used, the polynomial function can capture asymptotic conditions discussed above; yet, the power model requires an accumulation shutoff criterion; for example, the soil ceases accumulating the plastic strain when the cyclic strain drops below the elastic threshold strain or when the void ratio reaches the terminal void ratio (Pasten et al. 2014). Power models have been used extensively in pavement engineering whereby the cumulative strain in the *i*th cycle is related to the plastic strain in the first cycle and the power of the cycle number $\varepsilon_i = \varepsilon_1 i^c$ (see references in Table 1).

Log-linear function

The three-parameter log-linear function has been frequently used in the literature as well (references in Table 1). This model requires a shutoff condition in numerical simulations to capture terminal density (in volumetric strains) or shakedown (in shear strain accumulation).

Fig. 2. Void ratio evolution during repetitive loading versus number of cycles for (*a*) blasting sand, (*b*) Ottawa F110 sand, and (*c*) Ottawa 50–70 sand. The vertical cyclic stress amplitude is $\Delta\sigma'_v = 100$ kPa in all cases. Plots highlight the effect of the initial static load and the initial packing density on void ratio change during repetitive loading. Data are fitted with the polynomial model to estimate the terminal void ratio as the number of cycles $i \rightarrow \infty$. [Color online.]

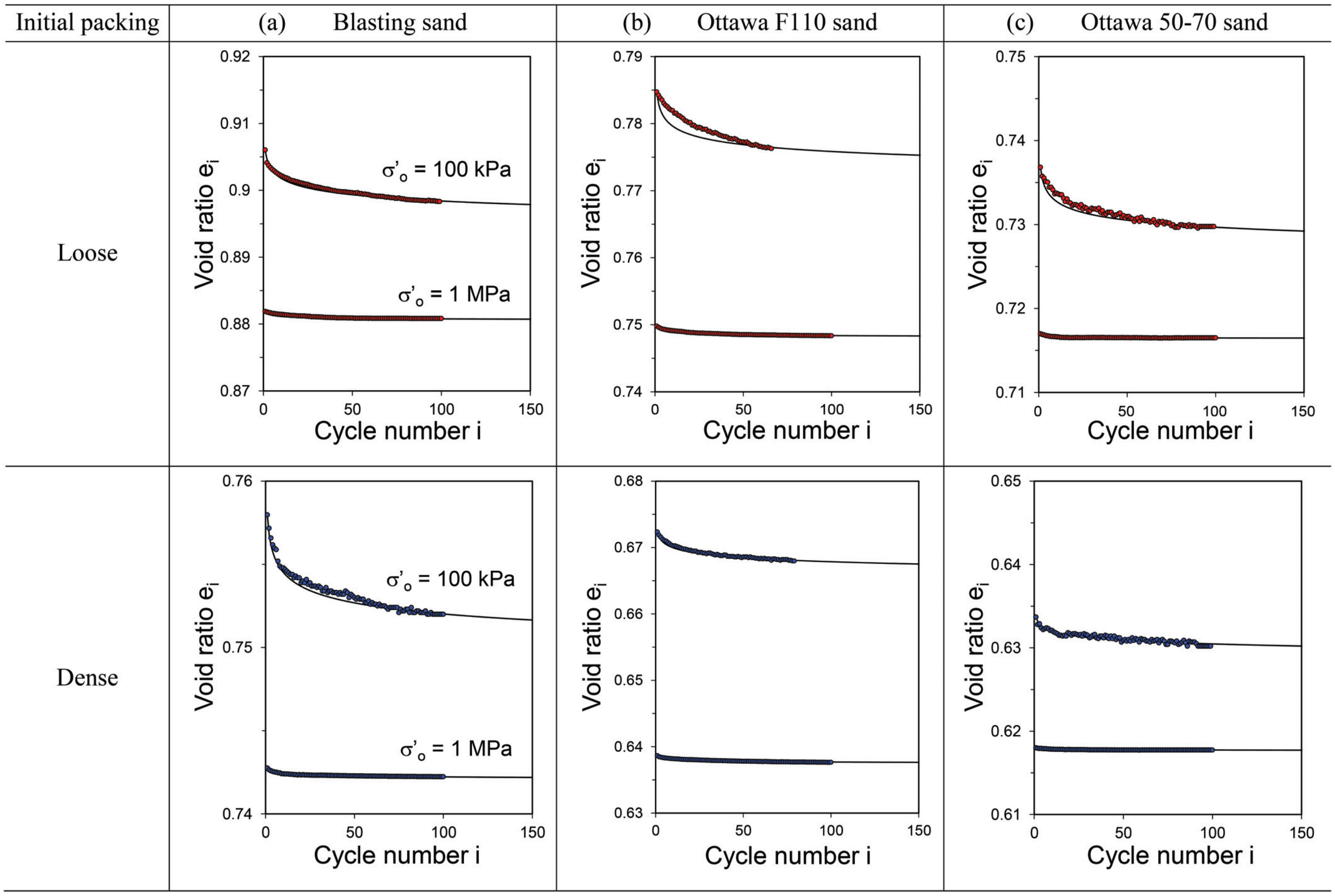

Experimental study

The experimental study consisted of vertical load cycles imposed onto sand specimens housed in a zero lateral strain oedometer cell. Three sands of different particle shape were packed at different initial densities. The static load was either $\sigma'_o = 100$ kPa or 1 MPa and the vertical repetitive stress amplitude was kept constant in all cases at $\Delta\sigma'_v = 100$ kPa. Sample preparation, devices, and procedures are described next.

Selected sands – sample preparation

The three selected sands were blasting sand, Ottawa F110, and Ottawa 50–70; their main characteristics are summarized in Table 2. Loose specimens were formed using the funneling method. Dense specimens were prepared by pouring and tamping successive soil layers.

Test devices

The oedometer cell (inner diameter = 72 mm and outer diamater = 83 mm) sits on the loading frame during sample preparation. Emphasis was placed on minimizing vibrations throughout the test. The vertical displacement was recorded continuously using a linear variable displacement transducer (LVDT) mounted on the top cap. The radial strain due to the repetitive load was $\varepsilon_r \sim 2 \times 10^{-6}$ and it satisfied the strain criterion $\varepsilon_r < 5 \times 10^{-5}$ recommended for k_o-studies (Okochi and Tatsuoka 1984).

System compliance

Deformation measurements may be biased by system compliance (Jardine et al. 1984; Jamiolkowski et al. 1994). System compliance is quantified carefully by using a steel dummy to measure the compression of porous stones and preferential compression at interfaces. The deformation amplitude for $\Delta\sigma'_v = 100$ kPa is 10^{-3} mm. This is subtracted from soil data to estimate the volumetric response of the soil mass.

Test procedure

Loose and dense specimens formed with all sands were subjected to "monotonic–repetitive-monotonic" loading stages where repetitive loads were applied at either low or high static loads:

- *Low static load* — Monotonic to 100 kPa → Repetitive: 200 kPa … 100 kPa → Monotonic to 1.4 MPa.
- *High static load* — Monotonic to 1 MPa → Repetitive: 1.1 MPa … 1 MPa → Monotonic to 1.4 MPa.

The repetitive load had a period of 20 s to avoid dynamic effects and to allow for short-time relaxation. The final monotonic load showed the load–deformation sediment response after repetitive loading. Complementary "monotonic" tests were conducted on fresh specimens by gradually loading identically formed specimens to 1.4 MPa.

Results

Figure 1 presents results for the 12 monotonic–repetitive–monotonic test sequences. Data for the six complementary mono-

Fig. 3. Evolution of the cumulative volumetric strain under k_o repetitive loading. Case: loose blasting sand at σ'_o = 100 kPa and at σ'_o = 1 MPa initial vertical stress; the vertical cyclic stress amplitude is $\Delta\sigma'_v$ = 100 kPa in both cases. Data (shown every other point) are fitted with selected strain accumulation models listed in Table 1. Mean proportional errors tabulated above show the best two fitted models; these are superimposed on the data. (Note: superscripts in the definition of the L2 norm are m for measured and p for predicted strain values (ε_u) at each cycle u and the total number of cycles is N = 100.) [Color online.]

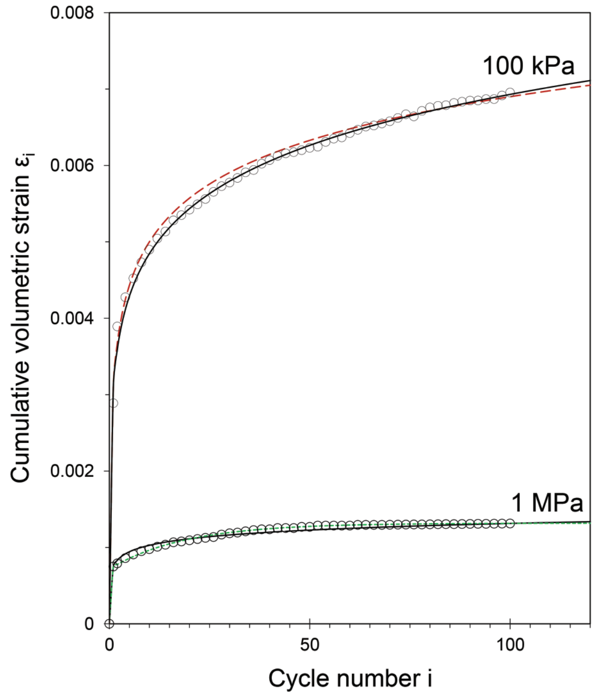

Initial stress	Exponential	Hyperbolic	Polynomial	Power	Log-Linear	Values for L2 -norm:
100 kPa	0.063	0.029	0.044	**0.014**	**0.018**	$\sqrt{\frac{1}{N}\sum_{u=1}^{N}\left(\frac{\varepsilon_u^m-\varepsilon_u^p}{\varepsilon_u^m}\right)^2}$
1 MPa	**0.012**	0.060	0.060	**0.028**	0.030	

tonic tests are not shown for clarity, but their overall trends overlap on the e–σ' response (where e is void ratio and σ' is the cyclic stress) for the monotonic–repetitive–monotonic tests shown in the figure. The wide scale used in these plots reflects the extreme void ratios e_{max} and e_{min} for these sands. The initial monotonic load produces most of the volume contraction in monotonic–repetitive–monotonic test sequences. The monotonic loading stage imposed after repetitive loading converges asymptotically to the void ratio trend obtained in monotonic tests without repetitive cycles ("shoulders" after the repetitive loading stage are clearly seen in the six tests that involved 100–200 kPa cycles). The effects of cyclic strain accumulation are eventually overcome at high stress; this response resembles densification stiffening produced by other overconsolidation processes besides loading, such as creep and diagenesis.

Figure 2 focuses on the evolution of void ratio against the number of cycles for different static loads σ'_o and initial packing densities. Void ratio changes are more pronounced in loose sands and at low static load, i.e., when $\Delta\sigma'_v/\sigma'_o$ is large. Most of the volume contraction occurs during the early cycles in all cases; in other words, the change in void ratio per cycle de/di decreases with the number of loading cycles.

Figure 3 shows data for two cases plotted in terms of volumetric strain computed from the beginning of repetitive loading. Models listed in Table 1 are fitted to the data. Plastic strain accumulation under zero lateral strain boundary conditions must approach terminal density, hence the d factor that characterizes the rate of ratcheting is set to zero in all models. The normalized L2 norm of the proportional errors is tabulated for all models in Fig. 3, and the best two fitting models are superimposed on the data; the mean error is less than 6% in all cases.

Terminal void ratios, e_T, are estimated by fitting the 12 datasets using the polynomial function for volumetric strain accumulation (for d = 0), but written in terms of void ratio

$$(1)\qquad e_i = e_1 - (e_1 - e_T)(1 - i^{-c}) \qquad \text{for } c > 0$$

where the c exponent controls the rate of convergence towards the terminal void ratio. Fitting parameters are summarized in Table 3. It can be observed that

1. The rate of change in void ratio captured in the c exponent is higher in loose sands.
2. Terminal void ratios, e_T, are higher than the minimum void ratios, e_{min}, for all sands tested as part of this study. From eq. (1), the extent of void ratio change by the 100th cycle $(e_1 - e_{100})/(e_1 - e_T)$ depends on the c exponent: it is only $(e_1 - e_{100})/(e_1 - e_T) \approx 20\%$ for c = 0.05, but reaches 90% for c = 0.5. This analysis suggests that more cycles are needed to determine e_T for dense sands at high confinement than for loose sands (however, low cyclic strain accumulation at $i \rightarrow \infty$ is anticipated for dense sands).
3. Terminal void ratios, e_T, are correlated with void ratios at the end of the first load cycle, e_1, regardless of loading conditions: the linear fit $e_T = 0.987e_1$ has a high correlation $R^2 = 0.99$. This result is due in part to the fact that changes in void ratio are small from e_1

Table 3. Repetitive load model parameters. Data for all sands are fitted with the generalized polynomial model in terms of void ratio (eq. (1)).

Sand	σ'_v (kPa)	Initial density	Void ratio after first cycle, e_1	Terminal void ratio, e_T	c exponent
Blasting sand	100	Loose	0.906	0.888	0.12
(e_{min} = 0.70)		Dense	0.758	0.743	0.11
	1000	Loose	0.882	0.880	0.30
		Dense	0.743	0.742	0.12
Ottawa F110	100	Loose	0.785	0.765	0.13
(e_{min} = 0.56)		Dense	0.672	0.652	0.05
	1000	Loose	0.750	0.748	0.34
		Dense	0.639	0.637	0.19
Ottawa 50–70	100	Loose	0.737	0.719	0.12
(e_{min} = 0.55)		Dense	0.634	0.618	0.05
	1000	Loose	0.717	0.716	0.50
		Dense	0.618	0.617	0.14

Note: Vertical cyclic stress amplitude is $\Delta\sigma'_v$ = 100 kPa in all cases.

to e_T, and because the extent of repetitive loading $\Delta\sigma'_v/\sigma'_o$ manifests primarily in the first cycle, from $e_{i=0}$ to e_1. In other words, the terminal condition under zero lateral strain repetitive vertical loading retains memory of the initial fabric.

Discussion: estimation of maximum settlement due to repetitive loads

The maximum expected change in relative density, ΔD_T, during repetitive loading can be expressed in terms of the initial void ratio, $e_{i=0}$, and the terminal void ratio, e_T, relative to the range e_{max}–e_{min} for that sand

$$\Delta D_T = \frac{e_{i=0} - e_T}{e_{max} - e_{min}} \tag{2}$$

These values are plotted in Fig. 4 against the initial relative density, $D_{i=0} = (e_{max} - e_{i=0})/(e_{max} - e_{min})$ for the 12 tests conducted with the three different sands as part of this study. The slope could vary with the particle shape and stress ratio $\Delta\sigma'_v/\sigma'_o$. Results confirm that a higher cyclic amplitude relative to the static load $\Delta\sigma'_v/\sigma'_o$ and a looser initial relative density lead to higher volumetric contraction to reach terminal density during repetitive loading.

Most importantly, results for the three different sands define single trends in the dimensionless space. Albeit limited to only two levels of stress $\Delta\sigma'_v/\sigma'_o$ = 0.1 and 1.0, Fig. 4 suggests a general procedure for a first-order estimate of the maximum plastic strain accumulation that a sandy sediment will experience beneath a foundation subjected to an infinite number of cycles

1. Determine the sand extreme void ratios, e_{max} and e_{min}.
2. Measure the void ratio $e_{i=0}$ after the application of the static load, but before the cyclic load starts. Compute the initial relative density $D_{i=0} = (e_{max} - e_{i=0})/(e_{max} - e_{min})$.
3. Estimate the maximum change in relative density the sediment would experience, ΔD_T, from Fig. 4 as a function of the in situ relative density, $D_{i=0}$, and the normalized cyclic stress amplitude, $\Delta\sigma'_v/\sigma'_o$.
4. Compute the maximum plastic strain the sediment will experience due to repetitive loading when $i \to \infty$.

$$\varepsilon_T = \Delta D_T \frac{e_{max} - e_{min}}{1 + e_{i=0}} \tag{3}$$

The ultimate footing settlement due to repetitive loading is the integral in depth of vertical strains $\varepsilon_T(z)$.

Fig. 4. Relative density before repetitive loading (defined in terms of $e_{i=0}$, e_{max}, and e_{min}) versus the maximum anticipated change in relative density after an infinite number of cycles (defined in terms of the terminal void ratio, e_T). The vertical cyclic stress amplitude is $\Delta\sigma'_v$ = 100 kPa in all cases. Note: the terminal void ratios are obtained by fitting the polynomial model to the data (Table 3). [Color online.]

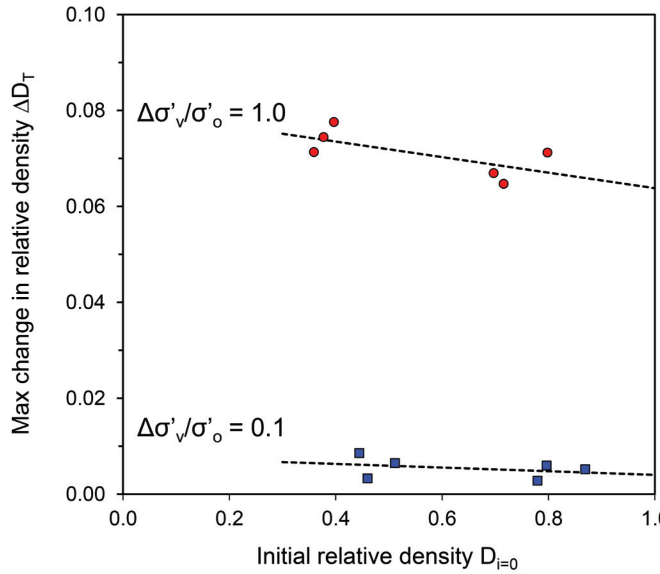

Definition	Equations
Initial relative density $D_{i=0}$	$D_{i=0} = \frac{e_{max} - e_{i=0}}{e_{max} - e_{min}}$
Max change in relative density ΔD_T	$\Delta D_T = \frac{e_{i=0} - e_T}{e_{max} - e_{min}}$

Example

Consider a sand subjected to $\Delta\sigma'_v/\sigma'_o$ = 0.1 (e_{max} = 0.9, e_{min} = 0.6, and $e_{i=0}$ = 0.75 so that $D_{i=0}$ = 0.5). From Fig. 4, the maximum change in relative density to reach the terminal void ratio is ΔD_T = 0.075. Then, the accumulated plastic strain will reach ε_T = 1.3% after an infinite number of load repetitions.

Observations

Note that the proposed method requires only the in situ void ratio under the static load, the values of e_{max} and e_{min} for the sand, and the amplitude of the repetitive load relative to the static load, $\Delta\sigma'_v/\sigma'_o$. While particle shape and grain-size distribution have a critical effect on the deformation of sands, their role is inherently taken into consideration in the proposed procedure through the values of e_{max} and e_{min} (Santamarina and Cho 2004; Cho et al. 2006).

Conclusions

Repetitive loads can negatively affect the long-term performance of geostructures. Previously suggested and new plastic strain accumulation models are generalized to include the plastic strain in the first cycle and to satisfy asymptotic conditions in volumetric strain (i.e., terminal density) and shear strain (i.e., shakedown and ratcheting). Exponential, polynomial, power, and hyperbolic models involve four parameters. The power model and the log-linear model have three model parameters, but require an accumulation shutoff criterion to capture either terminal density or shakedown.

New experimental results show the response of various sands, packed under both loose and dense conditions when subjected to repetitive vertical loading under zero lateral strain. The accumulation of plastic volumetric strain is more pronounced during early load cycles. The sediment evolves towards terminal void ratio; the terminal void ratio is greater than the extreme $e_{\min}$ in all cases tested in this study. Terminal void ratios are linearly correlated with initial void ratios at the beginning of repetitive loading; this implies that terminal conditions retain memory of initial conditions in soils subjected to repetitive vertical loading under zero lateral strain conditions.

Albeit limited, the dataset generated from this study suggests the possible development of a general chart and procedure for a first-order settlement estimation when shallow foundations are subjected to repetitive loading. The method is based on the concept of terminal void ratio. Its implementation requires the in situ void ratio under the static load, the values of $e_{\max}$ and $e_{\min}$ for the sand, and the ratio between the amplitude of the repetitive load and the initial static load, $\Delta\sigma'_v/\sigma'_o$.

Acknowledgements

This research was conducted by the authors while at the Georgia Institute of Technology. Support for this research was provided by the Goizueta Foundation and the KAUST endowment.

References

Abdelkrim, M., Bonnet, G., and de Buhan, P. 2003. A computational procedure for predicting the long term residual settlement of a platform induced by repeated traffic loading. Computers and Geotechnics, **30**(6): 463–476. doi:10.1016/S0266-352X(03)00010-7.

Achmus, M., Kuo, Y.-S., and Abdel-Rahman, K. 2009. Behavior of monopile foundations under cyclic lateral load. Computers and Geotechnics, **36**(5): 725–735. doi:10.1016/j.compgeo.2008.12.003.

Alonso-Marroquin, F., and Herrmann, H.J. 2004. Ratcheting of granular materials. Physical Review Letters, **92**(5): 054301. doi:10.1103/PhysRevLett.92.054301.

ASTM. 2014*a*. Standard test methods for maximum index density and unit weight of soils using a vibratory table. ASTM standard D4253-14. American Society for Testing and Materials, West Conshohocken, Pa. doi:10.1520/D4253-14.

ASTM. 2014*b*. Standard test methods for minimum index density and unit weight of soils and calculation of relative density. ASTM standard D4254-14. American Society for Testing and Materials, West Conshohocken, Pa. doi:10.1520/D4254-14.

Barksdale, R.D. 1972. Laboratory evaluation of rutting in basecourse materials. *In* Proceedings of the 3rd International Conference on Structural Design of Asphalt Pavements, London. pp. 161–175.

Bouckovalas, G., Whitman, R., and Marr, W. 1984. Permanent displacement of sand with cyclic loading. Journal of Geotechnical Engineering, **110**(11): 1606–1623. doi:10.1061/(ASCE)0733-9410(1984)110:11(1606).

Brown, S.F. 1974. Repeated load testing of a granular material. Journal of the Geotechnical Engineering Division, ASCE **100**(7): 825–841.

Brown, S.F. 1996. Soil mechanics in pavement engineering. Géotechnique, **46**(3): 383–426. doi:10.1680/geot.1996.46.3.383.

Chai, J., and Miura, N. 2002. Traffic-load-induced permanent deformation of road on soft subsoil. Journal of Geotechnical and Geoenvironmental Engineering, **128**(11): 907–916. doi:10.1061/(ASCE)1090-0241(2002)128:11(907).

Chang, C., and Whitman, R. 1988. Drained permanent deformation of sand due to cyclic loading. Journal of Geotechnical Engineering, **114**(10): 1164–1180. doi:10.1061/(ASCE)0733-9410(1988)114:10(1164).

Chen, K., Cole, J., Conger, C., Draskovic, J., Lohr, M., Klein, K., Scheidemantel, T., and Schiffer, P. 2006. Granular materials: packing grains by thermal cycling. Nature, **442**(7100): 257–257. doi:10.1038/442257a. PMID:16855580.

Cho, G.C., Dodds, J., and Santamarina, J.C. 2006. Particle shape effects on packing density, stiffness, and strength: natural and crushed sands. Journal of Geotechnical and Geoenvironmental Engineering, **132**(5): 591–602. doi:10.1061/(ASCE)1090-0241(2006)132:5(591).

D'Appolonia, D.J., and D'appolonia, E.E. 1967. Determination of the maximum density of cohesionless soils. *In* Proceedings of the 3rd Asian Regional Conference on Soil Mechanics and Foundation Engineering. Vol. 1, pp. 266–268.

D'Appolonia, D.J., Whitman, R.V., and D'appolonia, E.E. 1969. Sand compaction with vibratory rollers. Journal of the Soil Mechanics and Foundations Division, ASCE, **95**(1): 263–284.

Dennis, N.D., Jr., Qui, Y., and Elliott, R.P. 1999. Factors affecting the permanent deformation of subgrade soils. *In* Pre-failure Deformation Characteristics of Geomaterials: Proceedings of the Second International Symposium on Pre-Failure Deformation Characteristics of Geomaterials, Torino, Italy, 28–30 September Vol. 1, pp. 719–724.

Diyaljee, V.A., and Raymond, G.P. 1982. Repetitive load deformation of cohesionless soil. Journal of the Geotechnical Engineering Division, ASCE, **108**(10): 1215–1229.

Duncan, J.M., and Chang, C.Y. 1970. Non-linear analysis of stress and strain in soils. Journal of the Soil Mechanics and Foundations Division, ASCE, **96**(5): 1629–1653.

Fatemi, A., and Yang, L. 1998. Cumulative fatigue damage and life prediction theories: a survey of the state of the art for homogeneous materials. International Journal of Fatigue, **20**(1): 9–34. doi:10.1016/S0142-1123(97)00081-9.

Finn, W.D.L. 1981. Liquefaction potential: developments since 1976. In Proceedings of the International Conference on Recent Advances in Geotechnical Earthquake Engineering and Soil Dynamics. Session 2, pp. 655–681.

Finn, W.D.L., and Vaid, Y.P. 1977. Liquefaction potential from drained constant volume cyclic simple shear tests. *In* Proceedings of the 6th World Conference on Earthquake Engineering, New Delhi, India. Session 6, pp. 7–12.

François, S., Karg, C., Haegeman, W., and Degrande, G. 2010. A numerical model for foundation settlements due to deformation accumulation in granular soils under repeated small amplitude dynamic loading. International Journal for Numerical and Analytical Methods in Geomechanics, **34**(3): 273–296.

García-Rojo, R., and Herrmann, H.J. 2005. Shakedown of unbound granular material. Granular Matter, **7**(2–3): 109–118. doi:10.1007/s10035-004-0186-6.

Ishikawa, T., Sekine, E., and Miura, S. 2011. Cyclic deformation of granular material subjected to moving-wheel loads. Canadian Geotechnical Journal, **48**(5): 691–703. doi:10.1139/t10-099.

Jamiolkowski, M., Lancellotta, R., LoPresti, D.C.F., and Pallara, O. 1994. Stiffness of Toyoura sand at small and intermediate strain. *In* Proceedings of the 13th International Conference on Soil Mechanics and Foundation Engineering, New Delhi. Vol. 1, pp. 169–172.

Jardine, R.J., Symes, M.J., and Burland, J.B. 1984. The Measurement of soil stiffness in the triaxial apparatus. Géotechnique, **34**(3): 323–340. doi:10.1680/geot.1984.34.3.323.

Kaggwa, W., Booker, J., and Carter, J. 1991. Residual strains in calcareous sand due to irregular cyclic loading. Journal of Geotechnical Engineering, **117**(2): 201–218. doi:10.1061/(ASCE)0733-9410(1991)117:2(201).

Karg, C., François, S., Haegeman, W., and Degrande, G. 2010. Elasto-plastic long-term behavior of granular soils: modelling and experimental validation. Soil Dynamics and Earthquake Engineering, **30**(8): 635–646. doi:10.1016/j.soildyn.2010.02.006.

Knight, J.B., Fandrich, C.G., Lau, C.N., Jaeger, H.M., and Nagel, S.R. 1995. Density relaxation in a vibrated granular material. Physical Review E, **51**(5): 3957. doi:10.1103/PhysRevE.51.3957.

Koiter, W.T. 1960. General theorems for elastic-plastic solids. Amsterdam, the Netherlands.

Kondner, R.L. 1963. Hyperbolic stress-strain response: cohesive soils. Journal of the Soil Mechanics and Foundations Division, ASCE, **89**(1): 115–143.

Laloui, L., Nuth, M., and Vulliet, L. 2006. Experimental and numerical investigations of the behaviour of a heat exchanger pile. International Journal for Numerical and Analytical Methods in Geomechanics, **30**(8): 763–781. doi:10.1002/nag.499.

Lekarp, F., Richardson, I., and Dawson, A. 1996. Influences on permanent deformation behavior of unbound granular materials. Transportation Research Record: Journal of the Transportation Research Board, **1547**: 68–75. doi:10.3141/1547-10.

Lentz, R.W., and Baladi, G.Y. 1980. Simplified procedure to characterize permanent strain in sand subjected to cyclic loading. *In* Proceedings of the International Symposium on Soils under Cyclic and Transient Loading. Vol. 1, pp. 89–95.

Lentz, R.W., and Baladi, G.Y. 1981. Constitutive equation for permanent strain of sand subjected to cyclic loading. Transportation Research Record, **810**: 50–54.

Li, D., and Selig, E. 1996. Cumulative plastic deformation for fine-grained subgrade soils. Journal of Geotechnical Engineering, **122**(12): 1006–1013. doi:10.1061/(ASCE)0733-9410(1996)122:12(1006).

Luong, M.P. 1980. Stress-strain aspects of cohesionless soils under cyclic and transient loading. *In* Proceedings of the International Symposium on Soils under cyclic and Transient Loading, Rotterdam, the Netherlands, pp. 315–324.

Monismith, C.L., Ogawa, N., and Freeme, C.R. 1975. Permanent deformation characteristics of subgrade soils due to repeated loading. *In* Proceedings of the 54th Annual Meeting of the Transportation Research Board, Vol. 537, pp. 1–17.

Monismith, C.L., Hicks, R.G., Finn, F.N., Sousa, J., Harvey, J., Weissman, S., Deacon, J., Coplantz, J., and Paulsen, G. 1994. Permanent deformation response of asphalt aggregate mixes. Strategic Highway Research Program, National Research Council.

Morgan, K., and Ntambakwa, E. 2008. Wind turbine foundations behavior and design considerations. *In* Proceedings of the American Wind Energy Association Windpower Conference, Houston, Tex.

Narsilio, G.A., and Santamarina, J.C. 2008. Terminal densities. Géotechnique, **58**(8): 669–674.

Niemunis, A., Wichtmann, T., and Triantafyllidis, T. 2005. A high-cycle accumulation model for sand. Computers and Geotechnics, **32**(4): 245–263. doi:10.1016/j.compgeo.2005.03.002.

Okochi, Y., and Tatsuoka, F. 1984. Some factors affecting k_0 values of sand measured in triaxial cell. Soils and Foundations, **24**(3): 52–68. doi:10.3208/sandf1972.24.3_52.

Osipov, V.I., Bik, N.N., and Rumjantseva, N.A. 1987. Cyclic swelling of clays. Applied Clay Science, **2**(4): 363–374. doi:10.1016/0169-1317(87)90042-1.

Pasten, C., and Santamarina, J.C. 2011. Energy geo-storage — analysis and geomechanical implications. KSCE Journal of Civil Engineering, **15**(4): 655–667. doi:10.1007/s12205-011-0006-6.

Pasten, C., Shin, H., and Santamarina, J. 2014. Long-term foundation response to repetitive loading. Journal of Geotechnical and Geoenvironmental Engineering, **140**(4): 04013036. doi:10.1061/(ASCE)GT.1943-5606.0001052.

Paute, J.L., Hornych, P., and Benaben, J.P. 1996. Repeated load triaxial testing of granular materials in the French Network of Laboratories des Ponts et Chaussées. *In* Proceedings of the European Symposium Euroflex 1993, Portugal, 20–22 September 1993. pp. 53–64.

Pejon, O.J., and Zuquette, L.V. 2002. Analysis of cyclic swelling of mudrocks. Engineering Geology, **67**(1–2): 97–108. doi:10.1016/S0013-7952(02)00147-3.

Rosato, A.D., and Yacoub, D. 2000. Microstructure evolution in compacted granular beds. Powder Technology, **109**(1–3): 255–261. doi:10.1016/S0032-5910(99)00241-7.

Sánchez, M., Shastri, A., and Le, T.M.H. 2014. Coupled hydromechanical analysis of an underground compressed air energy storage facility in sandstone. Géotechnique Letters, **4**(2): 157–164. doi:10.1680/geolett.13.00068.

Santamarina, J.C., and Cho, G.C. 2004. Soil behaviour: the role of particle shape. *In* Proceedings of Advances in Geotechnical Engineering: The Skempton Conference, London, March.

Sawczuk, A. 1974. Shakedown analysis of elastic-plastic structures. Nuclear Engineering and Design, **28**(1): 121–136. doi:10.1016/0029-5493(74)90091-0.

Sawicki, A. 1994. Elasto-plastic interpretation of oedometric test. Archives of Hydro-Engineering and Environmental Mechanics, **41**(1–2): 111–131.

Sawicki, A., and Swidzinski, W. 1995. Cyclic compaction of soils, grains and powders. Powder Technology, **85**(2): 97–104. doi:10.1016/0032-5910(95)03013-Y.

Sharp, R., and Booker, J. 1984. Shakedown of pavements under moving surface loads. Journal of Transportation Engineering, **110**(1): 1–14. doi:10.1061/(ASCE)0733-947X(1984)110:1(1).

Silver, M.L., and Seed, H.B. 1971. Volume changes in sands during cyclic loading. Journal of the Soil Mechanics and Foundations Division, ASCE, **97**(9): 1171–1182.

Stewart, H.E. 1986. Permanent strains from cyclic variable-amplitude loadings. Journal of Geotechnical Engineering, **112**(6): 646–660. doi:10.1061/(ASCE)0733-9410(1986)112:6(646).

Suiker, A.S.J., and de Borst, R. 2003. A numerical model for the cyclic deterioration of railway tracks. International Journal for Numerical Methods in Engineering, **57**(4): 441–470. doi:10.1002/nme.683.

Tripathy, S., and Subba Rao, K. 2009. Cyclic swell–shrink behaviour of a compacted expansive soil. Geotechnical and Geological Engineering, **27**(1): 89–103. doi:10.1007/s10706-008-9214-3.

Viklander, P. 1998. Permeability and volume changes in till due to cyclic freeze/thaw. Canadian Geotechnical Journal, **35**(3): 471–477. doi:10.1139/t98-015.

Wang, Y.H., and Santamarina, J.C. 2007. Attenuation in sand: an exploratory study on the small-strain behavior and the influence of moisture condensation. Granular Matter, **9**(6): 365–376. doi:10.1007/s10035-007-0050-6.

Wichtmann, T., Niemunis, A., and Triantafyllidis, T. 2005. Strain accumulation in sand due to cyclic loading: drained triaxial tests. Soil Dynamics and Earthquake Engineering, **25**(12): 967–979. doi:10.1016/j.soildyn.2005.02.022.

Wichtmann, T., Niemunis, A., and Triantafyllidis, T. 2007. Strain accumulation in sand due to cyclic loading: drained cyclic tests with triaxial extension. Soil Dynamics and Earthquake Engineering, **27**(1): 42–48. doi:10.1016/j.soildyn.2006.04.001.

Wichtmann, T., Niemunis, A., and Triantafyllidis, T. 2010*a*. Strain accumulation in sand due to drained cyclic loading: on the effect of monotonic and cyclic preloading (Miner's rule). Soil Dynamics and Earthquake Engineering, **30**(8): 736–745. doi:10.1016/j.soildyn.2010.03.004.

Wichtmann, T., Niemunis, A., and Triantafyllidis, T. 2010*b*. On the determination of a set of material constants for a high-cycle accumulation model for non-cohesive soils. International Journal for Numerical and Analytical Methods in Geomechanics, **34**(4): 409–440. doi:10.1002/nag.821.

Wolff, H., and Visser, A.T. 1994. Incorporating elasto-plasticity in granular layer pavement design. Proceedings of the Institution of Civil Engineers – Transport, **105**(4): 259–272. doi:10.1680/itran.1994.27137.

Yeo, B., Das, B.M., Yen, S.C., and Puri, V.K. 1994. Permanent settlement of shallow foundation on sand due to cyclic loading. *In* Proceedings of the International Symposium on Pre-failure Deformation Characteristics of Geomaterials, Sapporo, Japan. Vol. 1, pp. 635–640.

Youd, T.L. 1972. Compaction of sands by repeated shear straining. Journal of the Soil Mechanics and Foundations Division, ASCE, **98**(7): 709–725.